INDIAN JOURNAL OF SCIENCE AND TECHNOLOGY

RESEARCH ARTICLE

Application of a Trellis Coded Modulation to Ameliorate the 5G Communication for Tropical Regions

Trilochan Patra[1]*, **Swarup Kumar Mitra**[2]

1 Assistant Professor, ECE Department, Dream Institute of Technology, Kolkata, 700104, India
2 Professor, ECE Department, MCKV Institute of Engineering, Howrah, 711204, India

OPEN ACCESS

Received: 24-10-2022

Accepted: 01-12-2022

Published: 05–01-2023

Citation: Patra T, Mitra SK (2023) Application of a Trellis Coded Modulation to Ameliorate the 5G Communication for Tropical Regions. Indian Journal of Science and Technology 16(1): 37-46. https://doi.org/10.17485/IJST/v16i1.2079

* **Corresponding author**.

trilochanpatra266@gmail.com

Funding: None

Competing Interests: None

Published By Indian Society for Education and Environment (iSee)

ISSN
Print: 0974-6846
Electronic: 0974-5645

Abstract

Objectives: To minimize the bit error rate and enhance the radio signal power by an application of the Trellis Coded Modulation (TCM) for the Fifth Generation (5G) technology in tropical regions. **Methods:** Various diversity techniques have been adopted to diminish the Bit Error Rate. A Communication link model has been proposed in this work and an STBC MIMO system (Space-Time Block Coding multiple-input multiple-output) has been applied to enhance the diversity gain and coding gain of the proposed model. The said model has been implemented in this work for tropical regions for increasing the radio signal power. **Findings:** The basic climatic feature of tropical regions is a heavy amount of rainfall throughout the year. Because of such rainfall, the radio signal power in these regions gets diminished, and the Bit Error Rate (BER) increases. By applying the proposed communication link model in the tropical regions the Bit Error Rate has been reduced. The values of the Bit Error Rate of the proposed model have been obtained for Rayleigh distribution, Rician distribution and various MIMO techniques. **Novelty:** A hardware co-simulation block and a 4x4 STBC MIMO has been developed with its subsequent verification on Xilinx Kintex-7 FPGA board.

Keywords: Bit error rate; MIMO Systems; Xilinx system generator; Trellis coded modulation; FPGA; Signal attenuation

1 Introduction

In order to make a further study of the Fifth Generation technology in the wireless communication system, the researchers have been trying heart and soul for a long time. In [(1)] a 36-quadrature amplitude modulation (QAM) heterodyne technique featuring nonlinear precoding with nonuniform symbol probabilities, called Nonlinear Coded Nonuniform Convolutional (NCNS)-QAM has been suggested. In [(2)] the application of a trellis coded modulation (TCM) and maximal ratio combining (MRC) has been applied to overcome the degradation of the information signal caused by fading and noise. In [(3)] an adaptive antenna grouping (AAG) according to channel state information in massive MIMO scenarios has been discussed. The rain attenuation gets enhanced significantly with the increase of operating frequency, rain density and operative

length of the path. As a result, the authenticity, attainability and functionality,of the transmission link have been reduced. In this way, the spectrum appears fruitless in 5G technology. In order to better the above phenomenon, the MIMO techniques have been applied to the wireless connection. A MIMO applies multiple antennas to both the transmission side and the reception side, and it is considered the most important 5G communication technology to maximize the power of the system. The Fifth Generation network applies millimetre waves to transfer a lot of data to the users[(4)]. In[(5)] the advanced version of the Fifth Generation technology requires new channel coding techniques which focus on reducing complexity and minimizing the bit error rate. Again in[(5)] the potential error correction coding schemes that can be utilized for 5G technology have been examined in terms of the bit error incidence and complexity. The performance of the coded MIMO system using a source of bit stream with high-priority, medium-priority, and low-priority classes is investigated and analyzed in[(6)]. The principal objective of[(7)] is to study the implementation of multilevel amplitude modulation forced by trellis coding in downlink non-orthogonal multiple-access channels for visible light (VLC) communications. The main purpose of[(8)] is to describe the channel testing process to minimize the issues associated with the higher values embedded in the transmitted signals. This process depends on the development of a consistent sample of the similarity and the lack of consistent tracking methods. In[(9)] a novel scheme for trellis-coded modulation combined with stochastic shaping (PS-TCM) in intensity modulation/direct detection (IM/DD) systems using generalized frequency division multiplexing (GFDM) has been presented.

From the studies of the previous research work on the 5G communication, it is obvious that neither an application of a trellis coded modulation nor an application of a MIMO technique has been adopted to overcome the impediments in tropical regions. The efficacy of this research paper relates to a design of the 5G Communication model with the help of a trellis coded flexibility and a MIMO process for tropical regions. In this research work, the trellis coded modulation (TCM) has been accepted for the proposed communication link model as the flexibility of the trellis coded modulation is considered an effective process to diminish the power required without enhancing the bandwidth[(2)], and this process develops the accuracy of the digital modulation system without reducing the data rate. In addition, having applied a TCM through an STBC MIMO method, the power efficacy and the phantom efficacy are also achieved. The stages depicted in the STBC MIMO system are exhibited in section 2.1.

Section 1 portrays the introduction portion. Section 2 illustrates the methodology portion. Section 3 exhibits the analysis of the result and discussion portion. Section 4 narrates the conclusion portion. References have been portrayed in section 5.

2 Methodology

2.1 STBC MIMO Systems

In an STBC MIMO system, a code name has been chosen, and a multiple input multiple output system of type 4x4 has been developed with the aforesaid code name[(10)]. To detect the variations, the space -time block coding MIMO of type 4x4 proposed by Alamouti space- time block coding of type 2x2, has been developed with the help of a construction symbol adopted by Walsh-Hadamard to point out an error. In this paper, four groups of symbols along with four transmitting antennas and four receiving antennas, have been adopted. An identical conception of transferring symbols out of senders has been used for the structure of an Alamouti STBC of type 4x4. After that, these symbols are greatly distorted by random combining or altering stage, and the symbols are then transmitted afresh. The analogous procedure is repeated for the other two antennas. Thereafter, this process is echoed in each message. Utilities of a multiple- input multiple-output technique seem inevitable. A MIMO technique is very effective in improving the volume of channels through many antenna settings. In a multiple input- multiple -output technique, the quality of data increases by a local multiplexer. Instead of what is stated above, the authentication of this technique has been improved by applying timing coding. Space-time block coding has also been chosen for the MIMO technique to maximize diversity benefits.

Suppose, I_{s1},I_{s2},I_{s3} and I_{s4} are the transferred symbols. At the 1st interval of time, the four symbols are transferred following a sequence. At the 2nd interval of time, the coded symbols like $I_{s2}*$,$-I_{s1}*$, $I_{s4}*$ and $-I_{s3}*$ are transferred. In the same way, $I_{s3}*$, $I_{s4}*$, $-I_{s1}*$ & $-I_{s2}*$ and I_{s4}, $-I_{s3}$, $-I_{s2}$ & I_{s1} are transferred in the 3rd and 4th intervals of time. Negative symbols and conjugates have been used here in order to change the orthogonally supported phase which is the principal characteristic of Quasi orthogonal space–time block code (QOSTBC). Following a similar process, data is transferred from four transiting antennas for four times. By applying the repeated rule of Walsh-Hadamard and the orthogonality of a 2x2 matrix of Alamouti transmission, a STBC transfer matrix of type 4x4 has been developed. The following steps display how the coded signals are transferred to detect variations.

Stage I: Choosing $I_{s'}$ as a 2x2 Alamouti transmission matrix of I_{s1} and I_{s2} symbols, the equation of the matrix stands as

$$I_{s'} = \begin{bmatrix} I_{s1} & -I_{s2}* \\ I_{s2} & I_{s1}* \end{bmatrix}$$

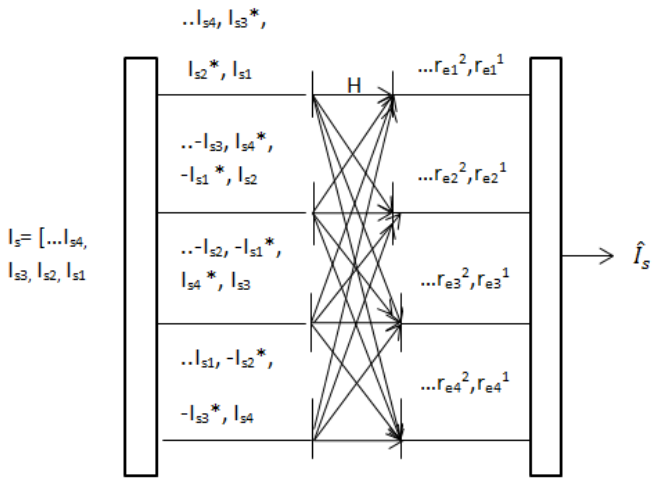

Fig 1. Diagram of MIMO Channel for 4x4 STBC Systems

Stage II: Selecting $I_{s''}$ as an group of another transference matrix for $I_{s3}I_{s4}$ symbols, the equation of the matrix stands as

$$I_{s''} = \begin{bmatrix} I_{s3} & -I_{s4}* \\ I_{s4} & I_{s3}* \end{bmatrix}$$

Stage III: Putting scalars back with matrixes in an Alamouti transference matrix of type 2x2 and naming again $I_{s'}$ and $I_{s''}$,

$$\begin{bmatrix} I_{s'} & -I_{s''}* \\ I_{s''} & I_{s'}* \end{bmatrix}$$

Stage IV: To achieve a 4x4 transfer matrix in the form of a 2x2 Alamouti matrix, the scalar values of matrixes are placed in with the help of a Hadamard matrix and the equations stand as

$$\begin{bmatrix} I_{s'} & -I_{s''}* \\ I_{s''} & I_{s'}* \end{bmatrix} \longrightarrow \begin{bmatrix} \begin{bmatrix} I_{s1} & -I_{s2}* \\ I_{s2} & I_{s1}* \end{bmatrix} & \begin{bmatrix} I_{s3} & -I_{s4}* \\ I_{s4} & I_{s3}* \end{bmatrix} \\ \begin{bmatrix} I_{s3} & -I_{s4}* \\ I_{s4} & I_{s3}* \end{bmatrix} & \begin{bmatrix} I_{s1} & -I_{s2}* \\ I_{s2} & I_{s1}* \end{bmatrix} \end{bmatrix} \longrightarrow \begin{bmatrix} I_{s1} & -I_{s2}* & -I_{s3}* & I_{s4} \\ I_{s2} & I_{s1}* & -I_{s4}* & -I_{s3} \\ I_{s3} & -I_{s4}* & I_{s1}* & -I_{s2} \\ I_{s4} & I_{s3}* & I_{s2}* & I_{s1} \end{bmatrix}$$

Stage V: To achieve an Quasi-Orthogonality,the signs for 2nd and 3rd columns have been altered as per equations displayed below-

$$\begin{bmatrix} I_{s1} & -I_{s2}* & -I_{s3}* & I_{s4} \\ I_{s2} & I_{s1}* & -I_{s4}* & -I_{s3} \\ I_{s3} & -I_{s4}* & I_{s1}* & -I_{s2} \\ I_{s4} & I_{s3}* & I_{s2}* & I_{s1} \end{bmatrix}$$

$$\longrightarrow \begin{bmatrix} I_{S1} & I_{S2}* & I_{s3}* & I_{S4} \\ I_{s2} & -I_{s1}* & I_{s4}* & -I_{s3} \\ I_{s3} & I_{s4}* & -I_{s1}* & -I_{s2} \\ I_{s4} & -I_{s3}* & -I_{s2}* & I_{s1} \end{bmatrix}$$

Finally, the transmission matrix is,

$$I_s = \begin{bmatrix} I_{s1} & I_{s2}* & I_{s3}* & I_{s4} \\ I_{s2} & -I_{s1}* & I_{s4}* & -I_{s3} \\ I_{s3} & I_{s4}* & -I_{s1}* & -I_{s2} \\ I_{s4} & -I_{s3}* & -I_{s2}* & I_{s1} \end{bmatrix}$$

Stage VI: The coded above symbols are now transmitted amidst the multiple input multiple output medium [11,12] the matrix of which stands as below-

$$\text{H}= \begin{bmatrix} h_{f11} & h_{f12} & h_{f13} & h_{f14} \\ h_{f21} & h_{f22} & h_{f23} & h_{f24} \\ h_{f31} & h_{f32} & h_{f33} & h_{f34} \\ h_{f41} & h_{f42} & h_{f43} & h_{f44} \end{bmatrix}$$

Now the input symbols connected with the aforesaid MIMO medium are influenced through noise till the input symbols arrive at the recipients. Additive White Gaussian (AWGN) noise is marked n_e. The matrixes demonstrated below exhibit the series of receivers in four intervals of time-

1st interval of time:

$$\begin{bmatrix} r_{e11} \\ r_{e21} \\ r_{e31} \\ r_{e41} \end{bmatrix} = \begin{bmatrix} h_{f11} & h_{f12} & h_{f13} & h_{f14} \\ h_{f21} & h_{f22} & h_{f23} & h_{f24} \\ h_{f31} & h_{f32} & h_{f33} & h_{f34} \\ h_{f41} & h_{f42} & h_{f43} & h_{f44} \end{bmatrix} \begin{bmatrix} I_{s1} \\ I_{s2} \\ I_{s3} \\ I_{s4} \end{bmatrix} + \begin{bmatrix} n_{e11} \\ n_{e21} \\ n_{e31} \\ n_{e41} \end{bmatrix}$$

2nd interval of time:

$$\begin{bmatrix} r_{e12} \\ r_{e22} \\ r_{e32} \\ r_{e42} \end{bmatrix} = \begin{bmatrix} h_{f11} & h_{f12} & h_{f13} & h_{f14} \\ h_{f21} & h_{f22} & h_{f23} & h_{f24} \\ h_{f31} & h_{f32} & h_{f33} & h_{f34} \\ h_{f41} & h_{f42} & h_{f43} & h_{f44} \end{bmatrix} \begin{bmatrix} I_{s2}* \\ -I_{s1}* \\ I_{s4}* \\ -I_{s3}* \end{bmatrix} + \begin{bmatrix} n_{e12} \\ n_{e22} \\ n_{e32} \\ n_{e42} \end{bmatrix}$$

3rd interval of time:

$$\begin{bmatrix} r_{e13} \\ r_{e23} \\ r_{e33} \\ r_{e43} \end{bmatrix} = \begin{bmatrix} h_{f11} & h_{f12} & h_{f13} & h_{f14} \\ h_{f21} & h_{f22} & h_{f23} & h_{f24} \\ h_{f31} & h_{f32} & h_{f33} & h_{f34} \\ h_{f41} & h_{f42} & h_{f43} & h_{f44} \end{bmatrix} \begin{bmatrix} I_{s3}* \\ I_{s4}* \\ -I_{s1}* \\ -I_{s2}* \end{bmatrix} + \begin{bmatrix} n_{e13} \\ n_{e23} \\ n_{e33} \\ n_{e43} \end{bmatrix}$$

4th interval of time:

$$\begin{bmatrix} r_{e14} \\ r_{e24} \\ r_{e34} \\ r_{e44} \end{bmatrix} = \begin{bmatrix} h_{f11} & h_{f12} & h_{f13} & h_{f14} \\ h_{f21} & h_{f22} & h_{f23} & h_{f24} \\ h_{f31} & h_{f32} & h_{f33} & h_{f34} \\ h_{f41} & h_{f42} & h_{f43} & h_{f44} \end{bmatrix} \begin{bmatrix} I_{s4} \\ -I_{s3} \\ -I_{s2} \\ I_{s1} \end{bmatrix} + \begin{bmatrix} n_{e14} \\ n_{e24} \\ n_{e34} \\ n_{e44} \end{bmatrix}$$

The expansion of matrixes depicted above signify the equations of a receiver.

The above equations of the receiver have also been displayed in term of matrixes in equation (3) –

$$\begin{bmatrix} r_{e1} \\ r_{e2} \\ r_{e3} \\ r_{e4} \\ r_{e1}* \\ r_{e2}* \\ r_{e3}* \\ r_{e4}* \end{bmatrix} = \begin{bmatrix} h_{f1} & h_{f2} & h_{f3} & h_{f4} \\ h_{f2} & -h_{f1} & h_{f4} & -h_{f3} \\ h_{f3} & -h_{f4} & -h_{f1} & h_{f2} \\ h_{f4} & h_{f3} & -h_{f2} & -h_{f1} \\ h_{f1}* & h_{f2}* & h_{f3}* & h_{f4}* \\ h_{f2}* & -h_{f1}* & h_{f4}* & -h_{f3}* \\ h_{f3}* & -h_{f4}* & -h_{f1}* & h_{f2}* \\ h_{f4}* & h_{f3}* & -h_{f2}* & -h_{f1}* \end{bmatrix} \begin{bmatrix} I_{s1} \\ I_{s2} \\ I_{s3} \\ I_{s4} \end{bmatrix} + \begin{bmatrix} n_{e1} \\ n_{e2} \\ n_{e3} \\ n_{e4} \\ n_{e1}* \\ n_{e2}* \\ n_{e3}* \\ n_{e4}* \end{bmatrix} \tag{3}$$

The above matrix is written as

$$r_e = \mathrm{H_{ef}} I_s + n_e \tag{4}$$

The above equation (4) has been expanded from equations (5)-(12) in the following manner .

$$r_{e1} = h_{f1} I_{s1} + h_{f2} I_{s2} + h_{f3} I_{s3} + h_{f4} I_{s4} + n_{e1} \tag{5}$$

$$r_{e2} = h_{f2} I_{s1} - h_{f1} I_{s2} + h_{f4} I_{s3} - h_{f3} I_{s4} + n_{e2} \tag{6}$$

$$r_{e3} = h_{f3} I_{s1} - h_{f4} I_{s2} - h_{f1} I_{s3} + h_{f2} I_{s4} + n_{e3} \tag{7}$$

$$r_{e4} = h_{f4}I_{s1} + h_{f3}I_{s2} - h_{f2}I_{s3} - h_{f1}I_{s4} + n_{e4} \tag{8}$$

$$r_{e1}* = h_{f1}*I_{s1} + h_{f2}*I_{s2} + h_{f3}*I_{s3} + h_{f4}*I_{s4} + n_{e1}* \tag{9}$$

$$r_{e2}* = h_{f2}*I_{s1} - h_{f1}*I_{s2} + h_{f4}*I_{s3} - h_{f3}*I_{s4} + n_{e2}* \tag{10}$$

$$r_{e3}* = h_{f3}*I_{s1} - h_{f4}*I_{s2} - h_{f1}*I_{s3} + h_{f2}*I_{s4} + n_{e3}* \tag{11}$$

$$r_{e4}* = h_{f4}*I_{s1} + h_{f3}*I_{s2} - h_{f2}*I_{s3} - h_{f1}*I_{s4} + n_{e4}* \tag{12}$$

The decoding process is shown below. The Maximal Ratio Combining (MRC) process is used here to obtain a complete CSIR (reduction data stream). Maximal ratio combining has consolidated the chosen coefficients which correspond to identical composite medium matrix[2] as depicted below:

$\widehat{I_s}$= $H_{ef}{}^{H}r_e$ which can be expanded in the form of equation (13) as displayed below-

$$\begin{bmatrix} \widehat{I_{s1}} \\ \widehat{I_{s2}} \\ \widehat{I_{s3}} \\ \widehat{I_{s4}} \end{bmatrix} = \begin{bmatrix} h_{f1} & h_{f2} & h_{f3} & h_{f4} & h_{f1}* & h_{f2}* & h_{f3}* & h_{f4}* \\ h_{f2} & -h_{f1} & -h_{f4} & h_{f3} & h_{f2}* & -h_{f1}* & -h_{f4}* & h_{f3}* \\ h_{f3} & h_{f4} & -h_{f1} & -h_{f2} & h_{f3}* & h_{f4}* & -h_{f1}* & -h_{f2}* \\ h_{f4} & -h_{f3} & h_{f2} & -h_{f1} & h_{f4}* & -h_{f3}* & h_{f2}* & -h_{f1}* \end{bmatrix} \begin{bmatrix} r_{e1} \\ r_{e2} \\ r_{e3} \\ r_{e4} \\ r_{e1}* \\ r_{e2}* \\ r_{e3}* \\ r_{e4}* \end{bmatrix} \tag{13}$$

The matrix as demonstrated in equation (13) can also be expanded in terms of equations from (14)-(17) below-

$$\hat{I}_{s1} = h_{f1}r_{e1} + h_{f2}r_{e2} + h_{f3}r_{e3} + h_{f4}r_{e4} + h_{f1}*r_{e1}* + h_{f2}*r_{e2}* + h_{f3}*r_{e3}* + h_{f4}*r_{e4}* \tag{14}$$

$$\hat{I}_{s2} = h_{f2}r_{e1} - h_{f1}r_{e2} - h_{f4}r_{e3} + h_{f3}r_{e4} + h_{f2}*r_{e1}* - h_{f1}*r_{e2}* - h_{f4}*r_{e3}* + h_{f3}*r_{e4}* \tag{15}$$

$$\hat{I}_{s3} = h_{f3}r_{e1} + h_{f4}r_{e2} - h_{f1}r_{e3} - h_{f2}r_{e4} + h_{f3}*r_{e1}* + h_{f4}*r_{e2}* - h_{f1}*r_{e3}* - h_{f2}*r_{e4}* \tag{16}$$

$$\hat{I}_{s4} = h_{f4}r_{e1} - h_{f3}r_{e2} + h_{f2}r_{e3} - h_{f1}r_{e4} + h_{f4}*r_{e1}* - h_{f3}*r_{e2}* + h_{f2}*r_{e3}* - h_{f1}*r_{e4}* \tag{17}$$

The equations from (5)-(17) stated above describe the device

2.2 Trellis Coded Modulation

The trellis codes for band-limited channels arise out of combining convolution coding with modulation. This state of combining is itself called trellis coded modulation (TCM). This form of signaling comprises two basic features-the first feature is that the number of signal points lying in the constellation utilized is greater than what is used for the modulation format of interest with the identical data rate. Here the surplus points allow the overhead of forward error control coding without giving up bandwidth. The second feature is the utilization of convolutional coding to introduce a certain authenticity between consecutive signal points. Therefore, only certain patterns or sequences of signal points are allowed[7]. TCM comprises an encoding function of

rate T = K_s / K_s + 1 and an M-ary display that directs M = 2^{K_s} input massages to a large constellation of M = 2^{K_s+1} point locations. K_s signifies the transferred bits.

If the transferred signal series{Sa} is contaminated by the Additive White Gaussian Noise (AWGN), the decoder will start to create the wrong decisions, and it may be involved in a trellis path consisting of multiple transmissions from the real path. Such errors are called incident events. If Viterbi decoding is applied, the probability of such error is estimated at a very high signal-to-noise ratio (SNR), and the probability of such error X' can be expressed mathematically as stated below-

$$X' \cong \text{NE free } W'\left(d_E \text{ free } /2\sigma'\right) \tag{18}$$

Where W′ denotes the Gaussian error integral. N_{Efree} denotes the average number of errors with distance $d_{E\ free}$. The free distance d_{Efree} of the trellis refers to the minimum Euclidean distance between pairs of sequences $\{S_a\}$ and $\{S_a'\}$ that the encoder generates and it is mathematically displayed below-

$$d_{\text{Efree}} = \min_{Sa \neq Sa'} \left[\sum_{m=1}^{M} \|S_a - S_a'\|^2\right]^{1/2} \tag{19}$$

2.3 Proposed Model

Having applied MATLAB and Xilinx system generator, the proposed communication link model has been developed. Diversity and coding gain are two input parameters that reflect the tropical channel characteristic in OSTBC and Trellis Coded Modulation. The flow chart of the proposed model has been described in 2.3.1 at the first instance. The description of the proposed communication link model has been illustrated in 2.3.2.

2.3.1 Algorithmic approach

This flow chart displays the high level composition of the suggested model of the communication link of the 4x4 STBC MIMO System in a step by step manner.

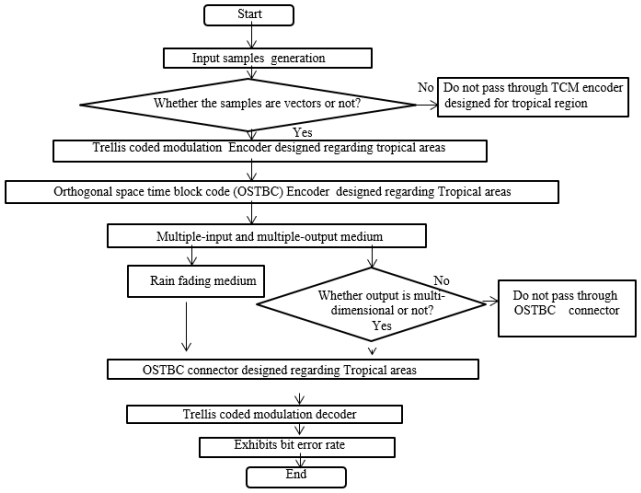

Fig 2. Flow chart of the proposed communication link model

2.3.2 Description of the proposed model

To reduce the bit error rate, a communication link model suggested in this paper as shown in Figure 3 below is endorsed for 5G technology in tropical areas. By applying the Xilinx System generator this proposed model has been bettered. The samples produced by the generator that yields binary numbers at random applying Bernoulli dispersion come out as vector output. Now the samples move along an unbuffer block changing the structure into a high-resolution sample. Later, the input samples make a passage along the 'Gateway In' block. This block alters the input of various Simulink numbers into a fixed Xilinx data-point. Then the data create a passage through the 'Gateway Out' block. The 'Gateway Out' block alters the input of a Xilinx constant bit into a

Simulink digital output. Then the output of data moves along a buffer block which transforms the scalar samples into an output structure of poor rate. Thereafter, the samples make a way through a trellis coded modulation encoder devised for tropical areas. An automatic gain controller is annexed to an encoder of a trellis coded modulation. This embedding is embedded into a binary data synchronization and harmonizes by an application of a phase shift switch technique. The TCM encoder has been designed in such a way that represents tropical areas.When the samples move through the encoder, the signal power remains strong for an addition of an automatic gain controller (AGC) with the TCM encoder. The input data, then go along the orthogonal space-time block code (OSTBC) encoder devised for tropical areas. Now the input information is encoded by dint of OSTBC. OSTBC contains a 1 ratio of two antennas, 1/2 or 3/4 of 3 and 4 antennas. At the time of moving the input messages along the orthogonal space-time block code encoder, the power of the signal continues to stay peak because the encoder is designed for this purpose. The input samples now make their way along a MIMO medium and this medium filtrates the samples with the MIMO multipath fading. Both the Rayleigh dissipation spreading and Rician dissipation spreading are included in the MIMO medium. From the MIMO medium the samples pass from end to end to the rain attenuation channel. When the signal travels along the passage of the rain fading channel, the power of the signal reduces. Now the input samples seek their path to go to the OSTBC connector. The inclusion of both the received signal and the channel estimate input must be commensurate with the OSTBC structure and the OSTBC connector brings about this phenomenon. This connector includes the signal obtained and the input of the channel limit in accordance with the OSTBC construction. The OSTBC connector is designed such that when the input samples make passage along the connector sample power increases. Then the input signal searches for a passage to reach the trellis coded modulation decoder. Now the decoder employs a Viterbi algorithm to ascertain the trellis coded modulation information that is adjusted by applying a phase switch technique. The input samples now proceed to the "error rate calculation block" that computes a percentage of the mistakes of the accepted data. A vector of three dimensions reflects the error block consisting of a percentage of the mistakes, the number of mistakes revealed and the symbols examined. The vector is now transferred to the workspace or outlet hole.

Bit error rate values rest on the various kinds of parameters such as the number of samples per frame, the number of transferring antennas for signal transfer and the number of receiving antennas for signals received. Bit error rate values also relies on the different types of fading dispersion. BER depending on the parameters used in this research work is highlighted in figures 6 and 7 shown below-

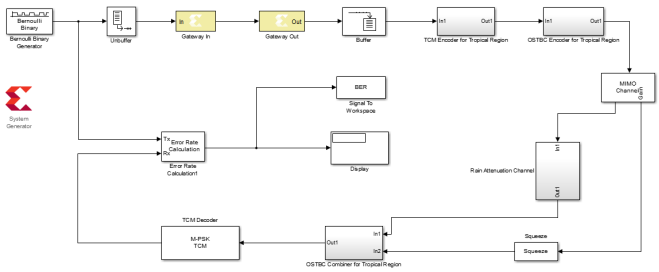

Fig 3. Suggested communication link model for 5G communication applying system generator

By using mathematical equations from (5) to (12) and from (14) to (17), an orthogonal space time block coding multiple-in multiple-out system of type 4x4 applied to the suggested link model has been developed with the application of a system generator and therefore, it is unavoidable to display the OSTBC MIMO model as shown below in Figure 4 . The system generator blocks consist of GatewayIn, GatewayOut, AddSub, Register, Constant and Mult. Simulink blocks comprising Signal generator and Scope. In Figure 4 , the OSTBC MIMO system is classified into three categories- a transmitter, a channel and a receiver. The transmitter contains the blocks signal generators, registers and GatewaysIn. A channel contains the blocks of a number of AddSub, Constant and Mult. A receiver comprises the blocks of GatewaysOut and Scopes. An OSTBC MIMO system plays a significant role in tropical regions as it reduces the signal loss and the BER of the radio signal to overcome the obstacles of these regions. In Figure 3 above an OSTBC MIMO system has been displayed in an OSTBC encoder for tropical regions.

3 Result and Discussion

The analysis of the result of the proposed model has been classified into two categories- hardware based result analysis and simulation based result analysis. The hardware based result analysis is described in 3.1 and the simulation based result analysis is illustrated in 3.2 noted below.

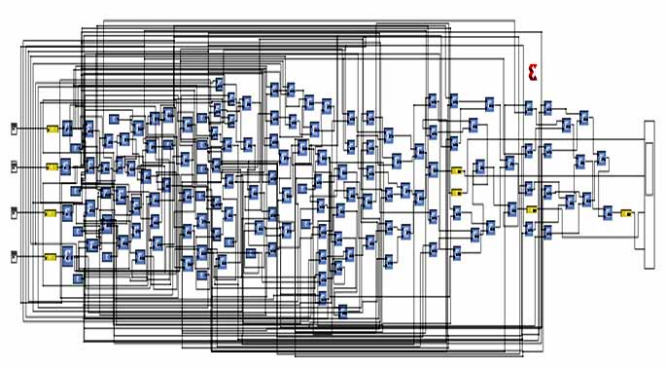

Fig 4. 4X4 OSTBC MIMO System model using system generator

3.1 Hardware based result analysis

A suggested model of the communication link that includes an orthogonal space-time block coding multiple input multiple output system of type 4x4 is executed in Xilinx kintex-7. Figures 5 and 6 show the device of hardware of the suggested model of communication link that includes an orthogonal space -time block coding multiple input multiple output system of type 4x4 with RTL Schematic vision and Schematic technology. HDL code is also used for modelling. A summary of device usage is listed below in Table 1 . In Table 1 , resource usage as shown appears to be very small. The outcome of low cost and power Systems-on-Chips (SoC) for a 4x4 OSTBC MIMO has been highlighted in Table 1 and Figure 7 shown below.The highest clock delay is 1.231000ns and the net skew obtained for the 4x4 MIMO design is 0.135000ns.

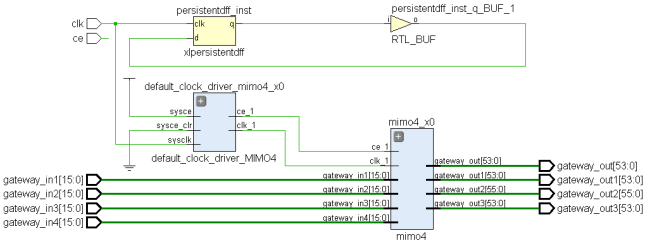

Fig 5. Simplified view relating to RTL for 4x4 OSTBC MIMO

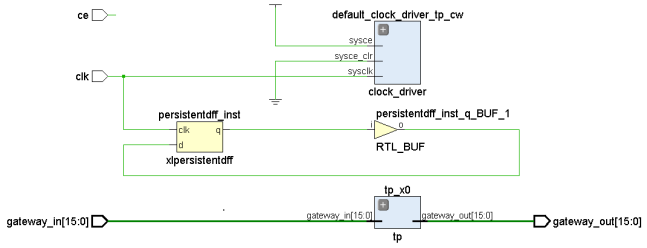

Fig 6. Simplified view relating to RTL for the model of communication link

3.2 Simulation based result analysis

The simulation results in respect of the suggested model for the communication link are analyzed in the following manner. When this suggested model undergoes simulation, the values of the BER get displayed in a block for Rayleigh dispersion and Rician dispersion. The values of the BER for two types of dispersions have been compared and Figure 8 quoted below shows this comparison in a graphical representation. Various

Table 1. Device utilization summary for Xilinx Kintex 7 FPGA Kit

Resources	Utilization	Available	Utilization %
Slice LUTs	2776	203800	1.36
A piece of the Registers	518	407600	0.13
Memory	2	445	0.45
DSP	33	840	3.93
IO	2	500	0.40
Clipping	4	32	12.50

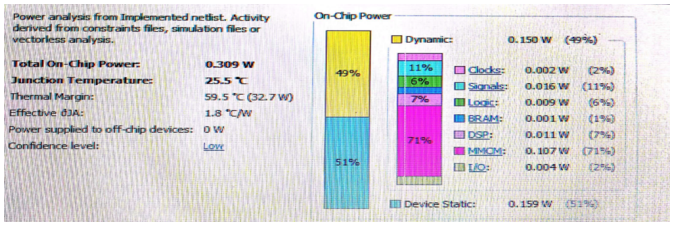

Fig 7. Power analysis of 4X4 OSTBC MIMO

kinds of MIMO technologies viz. 2x2, 3x3 and 4x4 are used in this suggested model. BER values for different MIMO strategies are shown in the aforesaid block of the suggested model, and a comparison of values of the BER for various multiplex-input and multiplex-output strategies exhibited in Figure 9 .

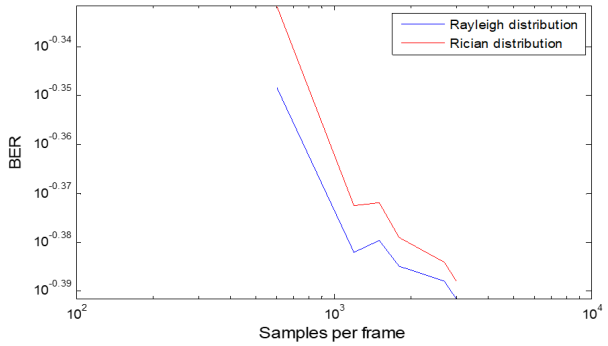

Fig 8. Graphical representation of bit error rate in respect of Rayleigh and Rician distributions

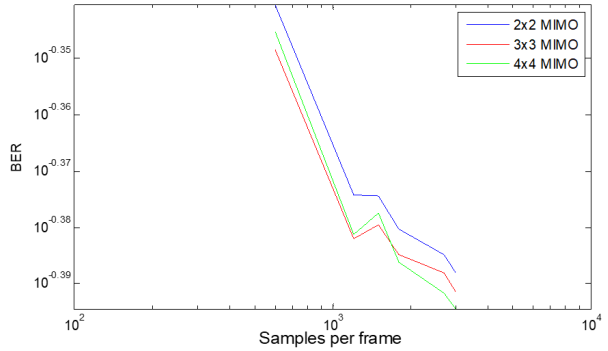

Fig 9. Graphical representation of bit error rate for various multiple-input and multiple-output system

All the previous research works included in the introduction portion have been examined but it would transpire that in some previous works trellis coded modulation has been used and in some works the 5G communication has been adopted. But it would appear that neither trellis coded modulation not 5G communication has been used for heightening the wireless communication system in tropical regions. So the work in this paper is quite different from the previous works. So there is left no scope for comparison between the previous works and the work in this. Besides, it would also appear that no hardware implementation of 4x4 OSTBC MIMO using Xilinx System generator and FPGA for tropical regions has been executed in the previous research works.

4 Conclusion

If this research work is depicted in a nut shell, it is observed from Figure 8 that Rayleigh fading produces less bit error rate than that produced by Rician fading. It would also appear from Figure 9 that a 4x4 MIMO technique yields less bit error rate than that rendered by MIMO techniques of lower order. As a result signal fading will be less by using Rayleigh distribution and 4x4 MIMO technique. The hardware design of the suggested model of a 4x4 OSTBC MIMO technique displays lower cost and lower power available from Table 1 and Figure 7. So the cost and power required for manufacturing a 4x4 OSTBC MIMO will be lower. In view of the observations stated above, it is concluded that the adoption of the suggested model can reduce the price and enhance the reliable power to develop the authenticity of the 5G technology in tropical areas. Therefore, it is anticipated that the proposed communication link model devised in this work will minimize the signal fading of radio signals in tropical regions and elevate the Fifth Generation communication system.

References

1) Zengyi X, Wenqing N, Jianyang S, Nan C. Nonlinear coded nonuniform superposition QAM by trellis-coding for MISO system in visible light communication. *Chinese Optics Letters*. 2022;20(4):1–6. Available from: https://opg.optica.org/col/abstract.cfm?URI=col-20-4-042501.
2) Baharuddin, Andre H, Muharam M, Luthfi A, Angraini R. Performance Analysis of Trellis Coded Modulation and Diversity Combining on Wireless Channel. *IOP Conference Series: Materials Science and Engineering*. 2021;1041(1):012023. Available from: https://doi:10.1088/1757-899X/1041/1/012023.
3) Chopra SR, Gupta A, Tanwar S, Safirescu CO, Mihaltan TC, Sharma R. Multi-User Massive MIMO System with Adaptive Antenna Grouping for Beyond 5G Communication Network. *Mathematics*. 2022;10(19):3621. Available from: https://doi.org/10.3390/math10193621.
4) Krasilov AN, Susloparov MV, Filatov OO, Khorov EM. Performance Evaluation of TCP Data Transmission in 5G mmWave Networks. *Journal of Communications Technology and Electronics*. 2020;65(6):735–740. Available from: https://doi.org/10.1134/S1064226920060194.
5) Mansingh P, Titus TJ, Yuvaraju M. BER Analysis of Channel Coding Techniques for 5G Networks. *1st International Conference on Science, Engineering and Technology (ICSET 2020), IOP Conf Series: Materials Science and Engineering*. 2020. Available from: .https://doi:10.1088/1757-899X/932/1/012091.
6) Mussawir AH. Error Performance Analysis of Wireless Video Communication Systems Employing Multi-level MPSK Modulation and MIMO Technologies. *European Journal of Engineering and Technology Research*. 2022;7(2):36–43. Available from: http://dx.doi.org/10.24018/ejeng.2022.7.2.2688.
7) Astharini D, Asvial M, Gunawan D. Performance of signal detection with trellis code for downlink non-orthogonal multiple access visible light communication. *Photonic Network Communications*. 2022;43(3):185–192. Available from: https://doi.org/10.1007/s11107-021-00957-5.
8) Albataineh Z, Hayajneh K, Salameh HB, Dang C, Dagmesh A. Robust massive MIMO channel estimation for 5G networks using compressive sensing technique. *International Journal of Electronics and Communications*. 2020;(120):153197–153203. Available from: https://doi.org/10.1016/j.aeue.2020.153197.
9) Feng T, Dong G, Xiangjun X, Zhang Q, Chuxuan W, Yongjun W, et al. Probabilistic shaped trellis coded modulation with generalized frequency division multiplexing for data center optical networks. *Optics Express*. 2019;27(23):33159–33169. Available from: https://doi.org/10.1364/OE.27.033159.
10) Han H, Caiyan L, Jun L, Yuyang P, Jia H, Xue-Qin J. Space-Time Block Coded Cooperative MIMO Systems. *Sensors*. 2020;21(1):1–11. Available from: https://doi.org/10.3390/s21010109.
11) Christopher ML. Performance of MIMO Systems Using Space Time Block Codes (STBC. 2021. Available from: https://doi.org/10.4236/ojapps.2021.113020.
12) Kawandal J, Pankaj V. Study of the STBC based MIMO System Modeling and Evaluation. *International Journal of Engineering and Innovative Technology*. 2021;11(4):1–4. Available from: https://www.ijeit.com/Vol%2011/Issue%204/IJEIT1412202110_01.pdf.